

Ag nanoclusters synthesized by successive ionic layer deposition method and their characterization

L. B. Gulina · G. Korotcenkov · B. K. Cho ·
S. H. Han · V. P. Tolstoy

Received: 6 November 2010 / Accepted: 29 January 2011 / Published online: 11 February 2011
© Springer Science+Business Media, LLC 2011

Abstract The possibilities of successive ionic layer deposition technology for synthesizing the Ag nanoclusters and nanolayers were analyzed in present article. It was shown that this technology, based on successive treatments of appropriate substrates in solution of cations and anions, is acceptable for the controllable forming of the Ag nanoparticles at the surface of different substrates. Results related to characterization of the Ag nanoclusters synthesized using $\text{Ag}(\text{NH}_3)_2\text{NO}_3$ or AgNO_3 precursors were discussed. It was found that the concentration and the size of the Ag nanoparticles deposited on a surface of fused quartz, silica gel, and monocrystalline silicon can be controlled by varying composition and pH of the reagent solutions as well as the number of the deposition cycles. It was established that the size of Ag nanoclusters depending on a synthesis conditions may vary from 1–5 nm to 500 nm. Model explained the growth of Ag clusters during successive ionic layer deposition was discussed as well.

L. B. Gulina · V. P. Tolstoy
St. Petersburg State University, St. Petersburg, Russia

G. Korotcenkov · B. K. Cho
Gwangju Institute of Science and Technology, Gwangju,
Korea

S. H. Han
Mokpo National Maritime University, Mokpo, Korea

G. Korotcenkov (✉)
Department of Materials Science and Engineering, GIST,
261 Cheomdan-gwagiro, Buk-gu, Gwangju 500-712, Korea
e-mail: ghkoro@yahoo.com

B. K. Cho (✉)
Department of Nanobio Materials and Electronics, GIST,
261 Cheomdan-gwagiro, Buk-gu, Gwangju 500-712, Korea
e-mail: chobk@gist.ac.kr

Introduction

Nanoclusters of Ag are currently objects of intensive research in the field of catalysis [1–6], electrochemical [7] and gas sensors [8–12], microelectronics, bio-applications [13], and nanocomposites [4, 6, 14–16]. Ag nanoclusters incorporated into either heterogeneous catalysts or gas sensing matrices considerably improve their respective operating parameters. For example, oxidation catalysts for carbon monoxide [2], H_2O_2 reduction [4], NO_x conversion [5], and numerous other volatile organic compounds (VOCs) [3] based on Ag are well known. For gas sensor applications, the most important effects of surface modification by Ag nanoclusters are the increase of sensitivity and the improvement of selectivity of sensor responses to specific analytes, such as H_2 and H_2S [8, 9]. Silicon porosification using metal-assisted chemical stain etching is another interesting area of Ag cluster application [17–19]. Noble metal nanoclusters, acting as local cathodes, while the areas surrounding these nanoclusters act as anodes, promote Si local etching and the formation of porous structures.

For Ag cluster synthesis or deposition, different methods such as impregnation [10, 20, 21], spray pyrolysis deposition, thermal evaporation [16], chemical vapor deposition (CVD), laser ablation, electrodeposition [7], magnetron sputtering [22], chemical decoration [4], solid-state reactions [23], photoinduced and photocatalytic reduction [15], thermal decomposition [24], and biosynthesis [13], among others, have already been demonstrated [5, 25–27]. In this article, we present results related to Ag cluster synthesis via the successive ionic layer deposition (SILD) method. The SILD method, taking into account its nature, is identical to methods such as successive ion layer adsorption and reaction (SILAR) [28, 29] and layer-by-layer (LBL) deposition [30].

However, we believe that the name SILD, which we use, fits better with the names of other methods of thin film synthesis, such as chemical vapor deposition (CVD), pulsed laser deposition (PLD), ion-beam assisted deposition (IBAD), and atomic layer deposition (ALD), etc., and more adequately reflects the essence of this method.

According to the SILD method, nanoparticles or nanolayers of an inorganic compound are formed on a substrate surface through a series of successive reactions of cation and anion adsorptions. During formation, the substrate surface is treated in solutions of salts such as acetates, chlorides, and the nitrates of various metals, with a necessary condition being the elimination of both excess reagents and reaction products from the surface. A more detailed description of the SILD method can be found in [31–33]. Previously, this method was successfully used to deposit nanolayers of metal sulfides [34], oxides, and hydroxides [31, 32, 34, 35]. The ability to accurately control the nanolayer thickness via the number of ionic deposition cycles is the main advantage of this technology [31]; the average thickness of metal-oxide layers after each deposition cycle is about 0.6–1.5 nm.

As it follows from the above description, the SILD technique is related to chemical deposition methods, which are among the most used techniques being applied for synthesizing Ag nanoparticles [4, 5, 14, 21, 25, 36]. However, it should be noted that, to date, there are no well-developed principles to control the size of Ag particles during their synthesis on the substrate surface. Indeed, research in this direction is yet in its initial stages and frequently has an empirical character. We believe that the SILD method discussed in this article should have the additional ability to control the size of Ag particles due to its multi-step process.

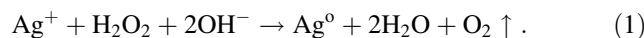
Previous experiments related to SILD technology have shown that the main problem of noble metal synthesis, in comparison with the synthesis of metal sulfides, is the fact that the synthesized layer consists of just one type of atoms. In this situation, it is difficult to select conditions of irreversible layer-by-layer adsorption of atoms at the second and each subsequent deposition cycles. However, during our research we found that this problem can be successfully resolved for metals (in particular for silver), for which the formation of Me^+ -type clusters during adsorption is possible.

Experimental details

Ag cluster synthesis

To synthesize Ag^0 nanolayers via the SILD method, the reduction reaction of silver cations in weakly alkaline solutions of hydrogen peroxide (H_2O_2) was chosen. It is

known [6] that upon being mixed, the interaction of these reagents forms a layer of metallic silver on the walls of the reaction vessel.



Plates of fused quartz, silica gel (Merk-60) with a specific surface area of $360 \text{ m}^2/\text{g}$, and substrates of monocrystalline Si (100) ($\rho \approx 40 \Omega \text{ cm}$) were used in this experiment. The quartz plates were successively treated in water, in concentrated nitric acid, in distilled water, in a solution of KOH with pH 9, and again in water before being used. Si wafers were first cleaned by acetone to degrease the Si surface. Next, the substrates were treated for 0.5 h under ultrasound impact ($P = 35 \text{ W}$) in a “piranha” solution, which presents a mixture of 30% H_2O_2 and concentrated H_2SO_4 in a 3:7 ratio, and then rinsed thoroughly with water to create a hydrophilic surface [37]. Such a preparation method is critical for SILD. After this treatment, a hydroxylated surface Si-OH is formed, which due to the presence of a negative charge at the surface is able to adsorb cations.

The synthesis of Ag on the substrates via SILD was carried out using the following procedure. During the first SILD cycle, substrates were treated in a metal salt solution (0.01 M solution of $\text{Ag}(\text{NH}_3)_2\text{NO}_3$) and samples were then washed with distilled water to remove the non-reacted reagents, treated with reductant, and again washed in distilled water. The silver ammine was prepared by adding in AgNO_3 solution of 0.1 M NH_4NO_3 and NH_4OH up to pH 8.5–9.0 of solution formed. A 0.1 M solution of ascorbic acid or a 0.3 M solution of $\text{H}_2\text{O}_2(\text{OH}^-)$ (both supplied by Vekton) was used as the reductant; the concentrations of solutions used were selected basing on previous experience. Time of processing with the $\text{Ag}(\text{NH}_3)_2\text{NO}_3$ solution and the time of the subsequent washing with water were 30 s each. Time of processing with the reductant solution and time of the subsequent washing with water were 1 min each. Such treatments represent the first deposition cycle.

During the following deposition cycles at the Ag^+ adsorption stage, solutions such as $\text{Ag}(\text{NH}_3)_2\text{NO}_3$ or AgNO_3 (analytical grade) were used. The first route was similar to the one described earlier. The second route included a series of treatments in AgNO_3 , H_2O , ascorbic acid, and H_2O_2 solutions. Parameters of the H_2O_2 treatment and washing were kept unchanged; these conditions were found to provide the maximum surface concentration of silver atoms deposited at the first cycle, as well as the maximum increment of nanolayer thickness in the subsequent SILD cycles. For Ag deposition, we used cycles between 1 and 12, as needed.

Structure and morphology characterization

To study the surface reactions during the process of Ag synthesis, spectroscopic methods of optical transmission

and diffusive dispersion in ultraviolet (UV) and infrared (IR) spectral regions were used. The choice of methods is conditioned by the fact that they allow Ag ions adsorbed at the surface to be identified. For example, spectra of diffusive dispersion in UV region provide an opportunity to identify Ag^+ ions; spectra in the visible region are used to identify metallic silver, and spectra overtones in the near infrared region (1,300–1,500 nm) can be used to identify free and bound hydrogen bond OH-groups on a silica surface, and then to establish how they change during the synthesis process. In the overtones region, the relative intensity of the absorption band of molecular water (1,450 nm) is considerably lower in comparison to the intensity of the absorption bands of the $\equiv\text{Si}-\text{OH}$ group (1,370 and 1,405 nm). FTIR spectra were obtained using a FTIR spectrometer Perkin-Elmer 1760X; the spectra are averages of 20–50 scans at a resolution of 4 cm^{-1} . In addition, the UV–Vis spectra were measured with a Lambda-9 spectrophotometer (Perkin-Elmer) at a scanning rate of 50 nm/min and a slit program of 2 nm.

A Zeiss EVO-40EP scanning electron microscope (SEM) with a LaB₆ cathode and accelerating voltage of 20 keV and a Veeco diNanoscopeV (with tapping mode tip RTESP 7, $f = 277 \text{ kHz}$) atomic force microscope (AFM) were used to characterize the sample morphology.

An X-ray diffraction (XRD) study of the Ag particles synthesized on the Si surface was carried out using a Thermo ARL X'TRA diffractometer (Cu K_α) in $\theta-\theta$ scanning mode at a fixed angle of incidence (2°).

Results and discussions

Transmission spectra of silver nanolayers synthesized on a fused quartz surface are shown in Fig. 1.

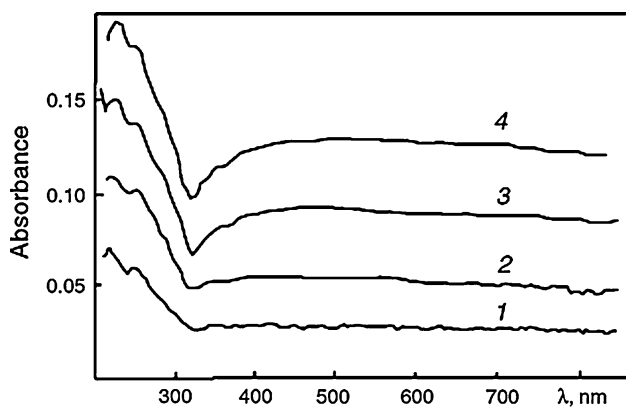


Fig. 1 Transmission spectra of a fused quartz substrate covered by nanolayers of metallic silver synthesized by 1, 2, 3, 6, 9, and 12 SILD cycles. Ag^0 nanoparticles were synthesized using $\text{Ag}(\text{NH}_3)_2\text{NO}_3$ and H_2O_2 solutions

These spectra show that repeated treatment of the substrate increases the nanolayer thickness on a fused quartz surface, as evidenced by the fact that an increasing number of cycles enhanced the absorption bands at 350–700 nm. According to [38], this band can be ascribed to Ag^0 clusters. In addition to the Ag^0 band, the band at 200–250 nm presents Ag^+ cations [39]. The Ag^+ band intensity increases remarkably after treating the sample in an AgNO_3 solution and washing with water. This observation was interpreted as being due to the non-reversible adsorption of silver cations on the surface. However, the subsequent treatment of the sample in a reductant solution suppresses but does not eliminate the Ag^+ band, possibly indicative of the incomplete reduction of the adsorbed silver cations. To further interpret the observed SILD regularities, the following model of the surface reactions was suggested [40]; treating the substrate in a solution of silver salt followed by washing with an ammonium solution produces adsorbed silver ammine according to following reactions:



However, the interaction of pre-adsorbed Ag^+ cations with a reducing agent is not complete and by-products such as Ag_2^+ or Ag_4^{2+} clusters are formed [41]. The presence of these species in the deposited nanolayer can be associated with the observed abrupt decrease in the intensity of the overtone absorption bands of free and H-bonded silanols at 1,370 and 1,400 nm, respectively (Fig. 2). It is also possible that positively charged silver clusters Ag_2^+ , Ag_4^{2+} , etc. are linked to the surface through the formation of

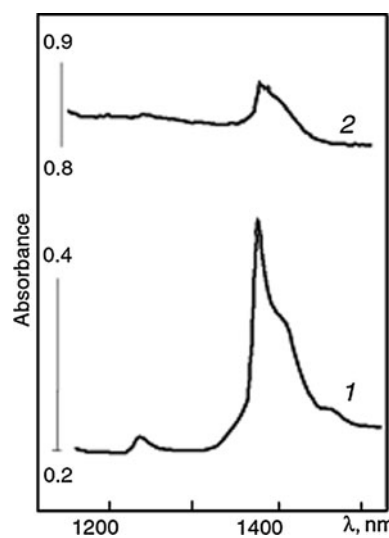


Fig. 2 Diffuse reflectance spectra of silica gel 1 before and 2 after synthesis of an Ag layer by one SILD cycle. Ag^0 nanoparticles were synthesized using $\text{Ag}(\text{NH}_3)_2\text{NO}_3$ and H_2O_2 solutions

complexes like $\equiv\text{Si}-\text{OAg}_2$ or $\equiv\text{Si}-\text{OAg}_4$. Note that the formation of such surface species is consistent with the spectral picture observed in the mid-IR region, which follows from the analysis of the Si–O stretching bands at 950 cm^{-1} .

These surface complexes can act as adsorption centers for silver cations during the following sample interaction with an AgNO_3 solution. The subsequent reduction of these enlarged complexes produces silver clusters of larger size. It is posited here that Ag^+ cations can migrate along the surface during both the washing stage, which follows conditioning of the substrate with an Ag^+ solution, and the reduction stage. This migration could explain the growth of nanoparticle size with an increasing number of SILD cycles. As a result, a nanolayer of metallic silver is formed after several SILD cycles.

Figure 3a shows the SEM image of large silver particles deposited via the silver ammoniate and H_2O_2 solutions. The average size of the particles is about 500 nm and they agglomerate from particles of 100–200 nm in size. When

silver nitrate and ascorbic acid solutions were used as reagents, the size of the nanoparticles deposited was 20–30 nm (Fig. 3b).

However, it should be noted that a detailed study of the formed layer morphology, made by AFM (see Fig. 4), shows that even in case of the Ag nanolayer forming from $\text{Ag}(\text{NH}_3)_2\text{NO}_3$ and H_2O_2 solutions, at the surface, both large particles and nanoclusters were formed. The nanoclusters were uniformly distributed along the square, and have sizes between 50 and 100 nm after 12 deposition cycles. The cluster size increases with an increasing number of deposition cycles.

According to the AFM data, the radius of the Ag particles is relatively diverse and can range between 47 and 100 nm (see Fig. 5). As shown in the figure, the ratio of the cluster width to its height could exceed 20 times.

The same situation was observed for layers formed using AgNO_3 and ascorbic acid solutions. As seen in Fig. 6, nanoparticles have a diameter of 5–30 nm and height of 1–5 nm; the average size of nanoparticles

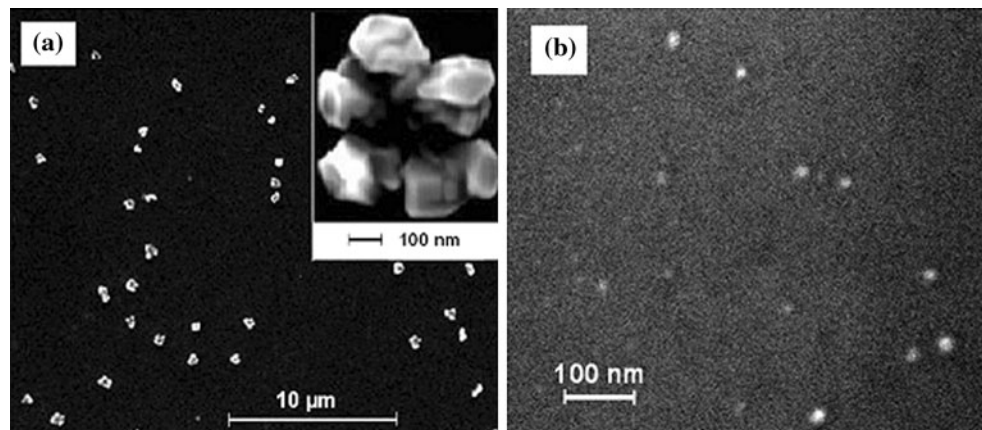


Fig. 3 SEM images of the silicon surface: **a** after synthesis of the Ag nanoparticles from $\text{Ag}(\text{NH}_3)_2\text{NO}_3$ and H_2O_2 solutions, $n = 5$; **b** after synthesis of the Ag nanoparticles from AgNO_3 and ascorbic acid solutions, $n = 5$

Fig. 4 AFM image of the Ag^0 layers synthesized on a silicon surface by **a** 1 and **b** 3 SILD cycles ($10\text{ }\mu\text{m} \times 10\text{ }\mu\text{m}$). Ag^0 nanoparticles were synthesized using $\text{Ag}(\text{NH}_3)_2\text{NO}_3$ and H_2O_2 solutions

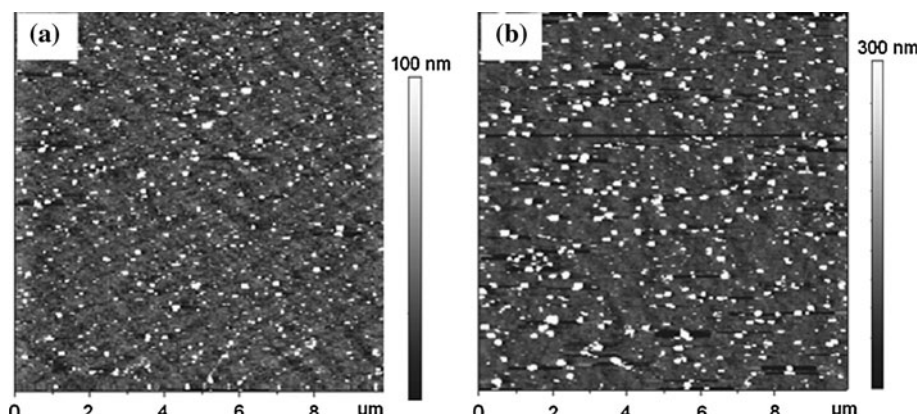


Fig. 5 Histograms of size distribution of Ag^0 nanoparticles synthesized on silicon surface by 1 SILD cycle. The scanned area was $8 \times 8 \mu\text{m}^2$. Ag^0 nanoparticles were synthesized using $\text{Ag}(\text{NH}_3)_2\text{NO}_3$ and H_2O_2 solutions

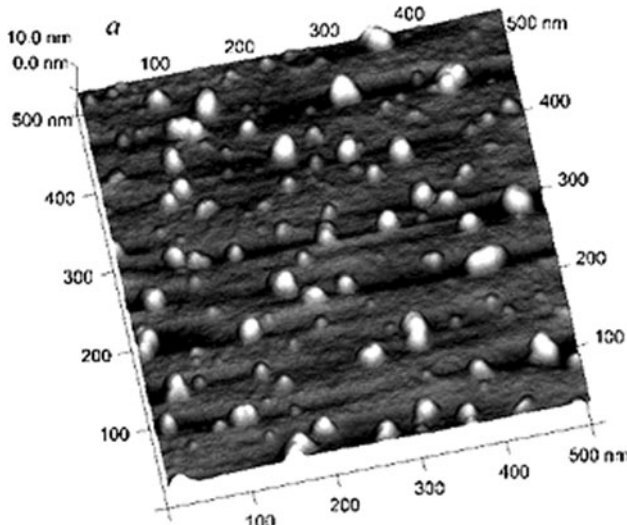
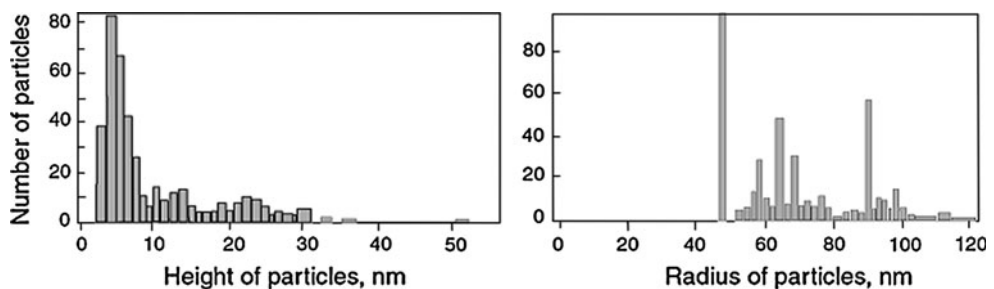


Fig. 6 AFM images of the Ag^0 nanoparticles synthesized on a silicon surface by 2 SILD cycles using solutions AgNO_3 and ascorbic acid ($500 \times 500 \text{ nm}$)

increases with increasing number of SILD cycles. However, the number of particles, observed at the surface after 1–5 deposition cycles, is being slightly changed. It is in accordance with conclusion made while studying the SnO_2 films synthesized by the SILD method [42]. According to Korotcenkov et al. [42], film growth during SILD takes place mostly through the growth of agglomerates. This same effect was observed while using $\text{Ag}(\text{NH}_3)_2\text{NO}_3$ and H_2O_2 solutions for the synthesis of Ag clusters. For comparison, the average size of Ag colloidal particles in hydrosols, obtained in water solutions via AgNO_3 restoration, is usually in the range of 10–150 nm [4, 25–27].

The XRD pattern of the Ag particles synthesized on the Si surface is shown in Fig. 7. It was found that pattern corresponds to diffraction from the (111) plane of Ag, with a cubic crystallographic structure [20]. The same situation was observed in [13, 25]. According to the XRD data presented in the figure, Ag grains have an average size of $\sim 9\text{--}10 \text{ nm}$.

The experimental data allowed us to present a simple model that describes the observed evolution of the Ag nanoparticle morphology (Fig. 8). According to this model, the formation of Ag^0 nanoparticles on the silicon surface

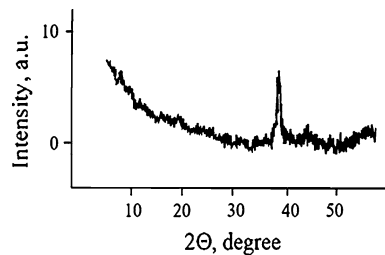


Fig. 7 XRD pattern of the Ag nanolayer synthesized on the Si surface (12 deposition cycles). Ag^0 nanoparticles were synthesized using $\text{Ag}(\text{NH}_3)_2\text{NO}_3$ and H_2O_2 solutions

takes place through two distinct stages. In the first stage, Ag^+ cations are adsorbed, being distributed uniformly at the surface. In the following reduction stage, the Ag^0 clusters are formed. Note that suggested growth mechanism is often employed to explain the growth of films when using chemical methods of deposition. By its nature, the suggested model is close to the diffusion limited aggregation model proposed by Witten and Sander [43] and the cluster–cluster aggregation model designed by Meakin [44].

According to the suggested model, at the initial stage 1-D clusters are being formed with following transformation in 2-D clusters, which afterward are being transformed in 3-D clusters with the increase of the number of deposition cycles. According to our estimations, when we use silver ammonium and H_2O_2 solutions, minimal size of 1-D cluster is $\sim 5\text{--}10 \text{ nm}$, and while using AgNO_3 and ascorbic acid solutions, minimal size of 1-D cluster is about 1–5 nm. Indicated above transformation of Ag particles from 1-D clusters to 3-D aggregates supposes that Ag^+ cations can migrate along the surface during the reduction process. This means that the $\equiv \text{SiO}-\text{Ag}^+$ bond is not strong. We need to note that the inclination to aggregation is well known features of Ag nanoparticles [5, 12, 27]. It was shown in many articles that silver tends to form big clusters on the support surface already at relatively low temperatures [12]. According to Ledo et al. [45], the fact that Ag 1-D clusters due to self-aggregation form 2-D islands and then 3-D aggregates can be related with the relative hydrophobic character of these 1-D clusters. Guillen-Villafuente et al. [46] have recently shown that Pt

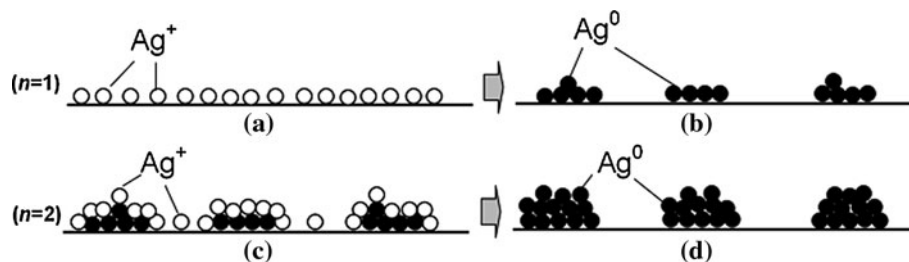


Fig. 8 Model of the Ag^0 nanoparticles formation on a substrate surface in the process of SILD. **a** after adsorption of the Ag^+ cations in the first SILD cycle, **b** after treatment with a reductant, **c** after

adsorption of the Ag^+ cations in the second SILD cycle, and **d** after treatment of sample **c** with a reductant

clusters prepared in microemulsions have also a tendency to self-aggregate when they are deposited onto the Au (111) surface forming ordered arrangements in several hierarchical levels.

The proposed nanoparticle growth model implies that SILD has considerable potential in controlling the surface density and the size of deposited metal nanoparticles since the SILD method employs separate and multiple stages of adsorption and reduction of cations. In the given model, the 1-D cluster's size probably should be determined by the number of the adsorption centers, formed on the surface of substrate, and by the concentration of Ag cations, adsorbed on the substrate surface during one deposition cycle. Such interpretation is in accordance with existing results. In particular, big size of the Ag particles synthesized using silver ammoniate and H_2O_2 solutions can be attributed to a relatively larger amount of Ag^+ cations adsorbed on a negatively charged surface of silicon oxide at higher alkaline pH. Then, the subsequent treatment with a reductant produces a larger amount of reduced Ag^0 atoms inclined to aggregation.

The chemical nature of the reductants used is also expected to affect the morphology of the silver nanoparticles. One can suppose that, as opposed to H_2O_2 , ascorbic acid adsorbs onto the Ag^0 nanoparticles and acts as a barrier that hinders from aggregation and growth of nanoparticles. At our point of view, besides indicated factors, the number of nucleation centers (defects) presented at the support surface should be of great importance as well. Just around those centers 2-D and 3-D clusters' forming takes place. This conclusion is in accordance with results presented in [47]. It was established that the metal oxide supports with higher defect density (TiO_2) results in smaller Ag cluster sizes at a higher dispersion.

Conclusions

Conducted research has shown that the SILD technology is acceptable for the controllable forming of the Ag nanoparticles at the surface of different substrates. For example,

under the SILD conditions, the concentration and the size of the Ag nanoparticles deposited on a surface of monocrystalline silicon can be controlled by varying composition and pH of the reagent solution as well as the number of the SILD cycles. As established, the size of the Ag nanoparticles depending on a synthesis conditions may vary from 1–5 nm for clusters to 500 nm for aggregates. This means that the SILD technology can be used for various purposes, requiring the presence of Ag nanoclusters at the support surface; in particular, either for the Si stain etching or for the surface modification of metal oxides aimed for gas sensor applications.

Acknowledgements This work was supported by Russian Foundation for Basic Research (RFBR) (Grant # 09-03-00892a), by the Korea Science and Engineering Foundation (KOSEF) grant funded by Ministry of Education, Science and Technology (MEST) (No. 2009-0078928), and by the World Class University (WCU) program at GIST through a grant provided by MEST, Korea (No. R31-20008-000-10026-0).

References

1. Imamura S, Ikebata M, Ito T, Ogita T (1991) Ind Eng Chem Res 30:217
2. Gulari E, Guldur C, Osuwani S, Srivannavit S (1999) Appl Catal A 182:147
3. Luo M, Yuan X, Zheng X (1998) Appl Catal A 175:121
4. Xu J, Wei XW, Song XJ, Lu XJ, Ji CC, Ni YH, Zhao GC (2007) J Mater Sci 42:6972. doi:[10.1007/s10853-006-1307-x](https://doi.org/10.1007/s10853-006-1307-x)
5. Sato T, Goto S, Tang Q, Shu Y (2008) J Mater Sci 43:2247. doi:[10.1007/s10853-007-1960-8](https://doi.org/10.1007/s10853-007-1960-8)
6. You X, Chen F, Zhang J, Anpo M (2005) Catal Lett 102(3–4):247
7. Song Y, Cui K, Wang L, Chen S (2009) Nanotechnology 20: 105501
8. Zhang J, Miremadi BK, Colbow KJ (1994) Mater Sci Lett 13: 1048
9. Tong MS, Dai GR, Wu YD, Gao DS (2000) J Mater Sci Mater Electron 11:661
10. Yamazoe N (1991) Sens Actuators B 5:7
11. Lu F, Chen S, Peng S (1998) Sens Actuators B 50:220
12. Zhang J, Colbow K (1997) Sens Actuators B 40:47
13. Govindaraju K, Basha SK, Kumar VG, Singaravelu G (2008) J Mater Sci 43:5115. doi:[10.1007/s10853-008-2745-4](https://doi.org/10.1007/s10853-008-2745-4)
14. Badr Y, Mahmoud MA (2006) J Mater Sci 41:3947. doi:[10.1007/s10853-005-5502-y](https://doi.org/10.1007/s10853-005-5502-y)

15. Alammar T, Mudring AV (2009) *J Mater Sci* 44:3218. doi: [10.1007/s10853-009-3429-4](https://doi.org/10.1007/s10853-009-3429-4)
16. Beyene HT, Chakravadhanula VSK, Hanisch C, Elbahri M, Strunskus T, Zaporozchenko V, Kienle L, Faupel F (2010) *J Mater Sci* 45:5865. doi: [10.1007/s10853-010-4663-5](https://doi.org/10.1007/s10853-010-4663-5)
17. Douani R, Si-Larbi K, Hadjersi T, Megouda N, Manseri A (2008) *Phys Status Solidi (a)* 205(2):225
18. Hadjersi T, Gabouze N (2007) *Phys Status Solidi (c)* 4(6):2155
19. Tsujino K, Matsumura M (2007) *Electrochim Acta* 53:28
20. Jiu J, Murai K, Kim D, Kim K, Suganuma K (2009) *Mater Chem Phys* 114:333
21. Qiu T, Wu XL, Shen JC, Ha PCT, Chu PK (2006) *Nanotechnology* 17:5769
22. Pierson JF, Rousselot C (2005) *Surf Coat Technol* 200(1–4):276
23. Jimenez JA, Lysenko S, Zhang G, Liu H (2007) *J Mater Sci* 42:1856. doi: [10.1007/s10853-006-0898-6](https://doi.org/10.1007/s10853-006-0898-6)
24. Uznanski P, Bryszewska E (2010) *J Mater Sci* 45:1547. doi: [10.1007/s10853-009-4122-3](https://doi.org/10.1007/s10853-009-4122-3)
25. Biju V, Sugathan N, Vrinda V, Salini SL (2008) *J Mater Sci* 43:1175. doi: [10.1007/s10853-007-2300-8](https://doi.org/10.1007/s10853-007-2300-8)
26. Zhou QF, Xu Z (2004) *J Mater Sci* 39:2487. doi: [10.1023/B:JMSC.0000020014.82696.85](https://doi.org/10.1023/B:JMSC.0000020014.82696.85)
27. Zhang W, Qiao X, Chen J (2007) *Mater Sci Eng B* 142:1
28. Fukui K, Nakane M (1995) *Sens Actuators B* 25:486
29. Salama T, Ohnishi R, Shido T, Ichikawa MJ (1996) *J Catal* 162:169
30. Decher G, Schlenoff JB (eds) (2003) *Multilayer thin films*. Wiley-VCH, New York
31. Korotcenkov G, Tolstoy V, Schwank J (2006) *Meas Sci Technol* 17:1861
32. Korotcenkov G, Cho BK, Han SD, Tolstoy V (2009) *Process Appl Ceram (Serbia)* 3(1–2):19
33. Tolstoy V (2006) *Russ Chem Rev* 75:161
34. Tolstoy VP, Murin IV, Reller A (1997) *Appl Surf Sci* 112:255
35. Tolstoy VP (1997) *Thin Solid Films* 307:10
36. Tsujino K, Matsumura M (2006) *Sol Energy Mater Sol Cells* 90(10):1527
37. Frantz P, Granick S (1992) *Langmuir* 8:1176
38. Karpov SV, Popov AK, Slabko VV, Shevina GB (1995) *Colloid J* 57(2):199
39. Ershov BG, Janata E, Henglein A, Fojtik AJ (1993) *Phys Chem* 97:4589
40. Tolstoy VP, Tolstobrov EV, Gulina LB (2002) *Vestnik SPbGU (Ser 4)* 3(20):120 (in Russian)
41. Janata E, Henglein A, Ershov BG (1994) *J Phys Chem* 98:10888
42. Korotcenkov G, Macsanov V, Tolstoy V, Brinzari V, Schwank J, Faglia G (2003) *Sens Actuators B* 96:602
43. Witten TA, Sander LM (1981) *Phys Rev Lett* 47:1400
44. Meakin P (1983) *Phys Rev Lett* 51:1119
45. Ledo A, Martinez F, Lopez-Quintela MA, Rivas J (2007) *Physica B* 398:273
46. Guillen-Villafuente O, Garcia G, Anula B, Pastor E, Blanco MC, Lopez-Quintela MA, Hernandez-Creus A, Planes GA (2006) *Angew Chem Int Ed* 45:4266
47. Lai X, St Clair TP, Valden M, Goodman DW (1998) *Prog Surf Sci* 59:25